The Binary Zoo: The Calculation of Production Rates of Binaries Through 2+1 Encounters in Globular Clusters

Melvyn B. Davies $\star$

Theoretical Astrophysics, Caltech, Pasadena CA 91125.

ABSTRACT

In studying encounters between binaries and single stars, one is interested in three classes of events: exchanges of stars, hardening of the original binary by a third star, and the production of merged objects. We present a means for computing cross sections for these three outcomes for an arbitrary binary and single star as might be found in the core of a globular cluster. The cross sections for a number of binaries in various stellar populations are then computed. We consider multiple encounters and the ultimate fate of a population of binaries fed into the cores of different globular cluster models. We see that the presence of only a relatively small number of binaries (containing 10% of the stars) will boost the production rate of astrophysically-interesting objects by a factor of at least a few over the rates expected from encounters between single stars. In particular, the ratio of smothered neutron stars to low-mass X-ray binaries (LMXBs) may be greatly increased, possibly explaining, in part, the excess of millisecond pulsars compared to LMXBs.

Key words: stellar: evolution – globular clusters

INTRODUCTION

Encounters involving binaries may be important in globular clusters even if their relative fraction is low, owing to their large cross section. When considering the evolution of dense stellar systems, and stellar encounters within them, one would therefore wish to account for encounters involving binaries, which may provide the energy source to support a core from collapse and may produce many of the stellar exotica seen; including blue stragglers, low-mass X-ray binaries (LMXBs), and millisecond pulsars (MSPs),

Encounters between binaries and single stars treating the stars as point masses have been considered in numerous works (Hut 1994, and references contained therein). Some allowance has also been made for the finite size of the stars in three-body simulations (see for example, Sigurdsson & Phinney 1994). Cleary & Monaghan (1990), and Davies, Benz & Hills (1993, 1994) also considered the hydrodynamical effects by performing some encounters using a smoothed particle hydrodynamics (SPH) code.

Studies of encounters between binaries and single stars show three main outcomes: the incoming star replaces one of the original components forming a new, detached, binary in a so-called *clean exchange*, the incoming star simply hardens

$\star$ Current Address: Institute of Astronomy, Madingley Road, Cambridge CB3 OHA

the binary without any exchange occuring – a so-called fly-by, or a merger between two of the stars occurs. One would wish to have expressions for these three outcomes; the exchange cross section, σ_{cx}; the fly-by cross section, σ_{fb}; and the cross section to form a merged object, σ_{mb}. The last outcome bifurcates; the merged object may be bound to the third star, producing a so-called *merged binary* (MB), or it may be unbound, an event that has been dubbed a *scattering-induced merger* (SIM).

We seek a means for computing these cross sections for various stellar masses, binary separations, and relative velocities. Rather than consider the three stellar masses, we can consider two mass ratios; the ratio of the secondary to the primary in the original binary, q_1, and the ratio of the incoming field star to that of the primary mass, q_2. We performed a series of three-body encounters for a range of mass ratios, q_1, q_2, and from them derived a number of parameters used to calculate the various cross sections. We then apply these cross sections, and feed various binaries into various stellar populations and compute the distribution of objects produced.

The parameters required to calculate the various cross sections are discussed in §2. The results of our three-body runs are given in §3. We apply these results in §4 and compute the various cross sections for various binaries in various stellar populations. We consider multiple encounters and the

Table 1. Parameters obtained for encounters involving circular binaries as a function of the ratio of the mass of the primary to the secondary in the original binary (q_1) and the ratio of field-star mass to the mass of the primary (q_2). See text for definitions of the parameters.

q_1	q_2	k_{ex}	k_{fb}	k_{12}	k_{13}	k_{23}	γ_{12}	γ_{13}	γ_{23}
0.312	2.000	45832	13747	36150	48099	29767	0.850	1.060	0.822
0.312	1.500	33231	10137	21193	22754	32566	0.772	0.880	0.967
0.312	1.000	17141	8108	24370	11412	24467	0.908	0.720	0.961
0.312	0.571	8151	4051	9265	7244	9335	0.626	0.564	0.708
0.571	2.000	31351	9517	27286	18589	23694	0.758	0.627	0.750
0.571	1.500	16849	3874	17623	14390	14373	0.756	0.626	0.665
0.571	1.000	11648	5354	12432	7600	12281	0.625	0.417	0.616
0.571	0.571	3187	4324	4965	4148	5147	0.451	0.412	0.540
1.000	2.000	19281	7853	16210	13000	13662	0.687	0.550	0.568
1.000	1.500	13104	5006	10941	10246	11370	0.566	0.531	0.594
1.000	1.000	6222	4883	5848	5030	5532	0.436	0.378	0.405
1.000	0.570	813	3370	3020	2360	2748	0.432	0.365	0.429

Table 2. Parameters obtained for encounters involving circular binaries as a function of the ratio of the mass of the primary to the secondary in the original binary (q_1) and the ratio of field-star mass to the mass of the primary (q_2). See text for definitions of the parameters.

q_1	q_2	k_{12x}	k_{13x}	k_{23x}	γ_{12x}	γ_{13x}	γ_{23x}	k_{12f}	k_{13f}	k_{23f}	γ_{12f}	γ_{13f}	γ_{23f}
0.312	2.000	12627	47205	29767	0.776	1.055	0.822	23944	0	0	1.017	0.000	0.000
0.312	1.500	8174	21812	32385	0.608	0.870	0.965	28975	0	0	1.324	0.000	0.000
0.312	1.000	9135	11078	23090	0.739	0.714	0.947	34157	0	0	1.483	0.000	0.000
0.312	0.571	4861	6814	7767	0.553	0.575	0.692	2544	302	431	0.699	0.433	0.745
0.571	2.000	3326	18563	23694	0.678	0.628	0.750	12520	0	0	0.921	0.000	0.000
0.571	1.500	8742	14061	13812	0.698	0.625	0.656	6901	456	0	0.788	0.833	0.000
0.571	1.000	5650	7382	11851	0.528	0.431	0.630	6109	212	183	0.836	0.228	0.319
0.571	0.571	1170	2472	2943	0.303	0.412	0.533	2959	1129	1407	0.555	0.432	0.555
1.000	2.000	6930	12892	14167	0.590	0.557	0.591	10785	78	33	0.912	0.446	0.000
1.000	1.500	4251	10224	10313	0.435	0.561	0.588	5972	154	939	0.767	0.178	0.795
1.000	1.000	2377	3771	4662	0.351	0.386	0.455	3238	681	569	0.684	0.340	0.284
1.000	0.570	242	581	847	0.317	0.345	0.469	1534	1227	1517	0.456	0.461	0.564

ultimate fate of binaries fed into particular globular clusters in §5.

2 THEORETICAL CROSS SECTIONS AND SCALING LAWS

The cross section for a single star to pass within a distance R_{min} of the center of mass of a binary is given by $\sigma = \pi R_{min}^2 (1 + V_c^2/V_\infty^2)$, where V_∞ is the relative speed at infinity, and V_c is the relative speed at which the system has zero total energy and is given by $V_c^2 = F(M_1, M_2, M_3)/d = GM_1 M_2(M_1 + M_2 + M_3)/M_3(M_1 + M_2)d$, where M_1 is the mass of the primary, M_2 the mass of the secondary and M_3 is the mass of the incoming, single star. In order for an exchange encounter to occur where the impacting star replaces one of the binary components, one might expect $R_{min} \sim d$, where d is the separation of the two components in the original binary. For a binary of separation ~ 10 AU, $V_c \simeq 10$ km/s (a typical value for the velocity dispersion in a globular cluster). Hence for hard binaries in globular clusters (where $d \sim 0.1 - 0.5$ AU), $V_c \gg V_\infty$, and the exchange cross section can be written as

$$\sigma_{ex} = k_{ex}(q_1, q_2)\pi d^2 \cdot \frac{GM_1 F(q_1, q_2)}{d} \cdot \frac{1}{V_\infty^2} \qquad (1)$$

where $q_1 = M_2/M_1$, $q_2 = M_3/M_1$, and $F(q_1, q_2) = q_1(1 + q_1 + q_2)/q_2(1 + q_1)$. The constant $k_{ex}(q_1, q_2)$ has to be determined through numerical simulations.

Similarly, one may write an expression for the cross section for fly-by encounters, where the components of the binary remain unchanged, but the binary is hardened by some minimum amount (taken to be 10% in our later calculations here).

$$\sigma_{fb} = k_{fb}(q_1, q_2)\pi d^2 \cdot \frac{GM_1 F(q_1, q_2)}{d} \cdot \frac{1}{V_\infty^2} \qquad (2)$$

where again $k_{fb}(q_1, q_2)$ has to be determined through numerical simulations.

One may also compute the cross section for two of the three stars to pass within some minimum distance during an encounter. Hut and Inagaki (1985) found that such a cross section can be written in the following form, for the ith and jth stars,

$$\sigma_{rmin}(i, j) = k_{rmin}(q_1, q_2, i, j)\pi d^2 \frac{GM_1 F(q_1, q_2)}{d} \cdot \frac{1}{V_\infty^2}$$

Table 3. Parameters obtained for encounters involving eccentric binaries as a function of the ratio of the mass of the primary to the secondary in the original binary (q_1) and the ratio of field-star mass to the mass of the primary (q_2). See text for definitions of the parameters.

q_1	q_2	k_{ex}	k_{fb}	k_{12}	k_{13}	k_{23}	γ_{12}	γ_{13}	γ_{23}
0.312	2.000	60643	15779	92862	31404	48135	0.906	0.799	0.832
0.312	1.500	38922	12143	52266	21366	25308	0.794	0.836	0.822
0.312	1.000	22535	9135	52055	18554	19072	0.897	0.823	0.725
0.312	0.571	9399	4711	13774	6189	7142	0.616	0.491	0.556
0.571	2.000	41067	10937	51170	25125	25297	0.720	0.672	0.643
0.571	1.500	26443	8517	32028	14190	19671	0.634	0.538	0.598
0.571	1.000	13536	5783	20371	11237	10781	0.619	0.518	0.521
0.571	0.571	4314	4656	8133	5003	5569	0.470	0.394	0.436
1.000	2.000	25546	8202	37341	15466	14579	0.699	0.523	0.526
1.000	1.500	16429	7539	22266	11558	12012	0.600	0.487	0.517
1.000	1.000	7328	5078	11315	7901	6093	0.501	0.461	0.364
1.000	0.571	1187	3896	4882	3184	3779	0.453	0.345	0.424

Table 4. Parameters obtained for encounters involving eccentric binaries as a function of the ratio of the mass of the primary to the secondary in the original binary (q_1) and the ratio of field-star mass to the mass of the primary (q_2). See text for definitions of the parameters.

q_1	q_2	$k_{12\mathrm{x}}$	$k_{13\mathrm{x}}$	$k_{23\mathrm{x}}$	$\gamma_{12\mathrm{x}}$	$\gamma_{13\mathrm{x}}$	$\gamma_{23\mathrm{x}}$	$k_{12\mathrm{f}}$	$k_{13\mathrm{f}}$	$k_{23\mathrm{f}}$	$\gamma_{12\mathrm{f}}$	$\gamma_{13\mathrm{f}}$	$\gamma_{23\mathrm{f}}$
0.312	2.000	39434	30488	49184	0.886	0.792	0.842	27707	0	0	0.855	0.000	0.000
0.312	1.500	27445	20883	24989	0.804	0.830	0.821	15966	0	0	0.720	0.000	0.000
0.312	1.000	24017	18057	19167	0.863	0.818	0.733	25629	0	0	1.092	0.000	0.000
0.312	0.571	6850	5283	6090	0.546	0.472	0.543	4546	481	1501	0.768	0.542	1.231
0.571	2.000	26972	24553	24917	0.679	0.668	0.641	14997	393	0	0.743	0.963	0.000
0.571	1.500	18230	13631	18970	0.609	0.533	0.601	12104	118	369	0.754	0.267	0.468
0.571	1.000	9125	10558	10262	0.526	0.530	0.543	8378	388	269	0.827	0.396	0.350
0.571	0.571	2394	2976	3223	0.396	0.384	0.429	4031	1359	1396	0.600	0.432	0.480
1.000	2.000	18656	15072	14023	0.627	0.525	0.525	11840	176	184	0.799	0.506	0.338
1.000	1.500	8246	10890	10846	0.478	0.493	0.512	11297	799	378	0.800	0.679	0.450
1.000	1.000	3337	6357	4312	0.389	0.490	0.360	4849	1277	919	0.600	0.459	0.319
1.000	0.571	506	900	1244	0.379	0.310	0.457	2854	1360	1455	0.514	0.396	0.416

$$\times \left(\frac{r_{\min}(i,j)}{d} \right)^{\gamma(i,j)} \tag{3}$$

where both $k_{\mathrm{rmin}}(q_1, q_2, i, j)$ and $\gamma(i, j)$ are to be determined (typically $\gamma(i, j) \sim 0.5$). We must find these constants for each of the three pairs; 1, 2; 1, 3; and 2, 3. We consider the three pairs separately to maintain generality; if two of the three stars are compact, we will not wish to consider close encounters between them (unless the binary separation is extremely small). We must also consider separately the cross section for encounters that contribute to either the exchange or fly-by cross section but which really led to some form of merger event. Again, we must consider each pair of stars separately. We thus have to compute *nine* values of k_{rmin} and γ.

To compute cross sections for mergers, we have to provide a value for the minimum distance, $r_{\min}(i, j)$, between the ith and jth stars. Here, we use the simple formula obtained by Kochanek (1992)

$$\frac{R_{\mathrm{merg}}}{R_i} = 1.7 \left(\frac{M_i + M_j}{2 M_i} \right)^{1/3} \tag{4}$$

where, for a given pair, the larger of the two values of R_{merg} is used.

We also have to differentiate between merger events leading to so-called merged binaries (MBs), where the merged object remains bound to the third star, and scattering induced mergers (SIMs), where the two objects are unbound. We may determine this branching ratio empirically for each set of simulations, thus having

$$
\begin{aligned}
\sigma_{\mathrm{sim}} &= \alpha_{\mathrm{sim}} \sigma_{\mathrm{rmin}} \\
\sigma_{\mathrm{mb}} &= (1 - \alpha_{\mathrm{sim}}) \sigma_{\mathrm{rmin}}
\end{aligned} \tag{5}
$$

where we have to compute an α for each of the three pairs of stars. We compute the cross sections in equation (4) for each of the three pairs and sum them (assuming all pairs contain no more than one compact star).

We compute the cross sections for *clean* exchanges by subtracting the cross section of exchanges that would really have led to merger events from the exchange cross section given in equation (1). We thus have

$$\sigma_{\mathrm{cx}} = \sigma_{\mathrm{ex}} - \sigma_{\mathrm{rmin|ex}} \tag{6}$$

where $\sigma_{\mathrm{rmin|ex}}$ is the cross section of merger events that were eroneously labelled as exchanges. Written out in full, $\sigma_{\mathrm{rmin|ex}} = i_{12}\sigma_{\mathrm{rmin|ex}}(1, 2) + i_{13}\sigma_{\mathrm{rmin|ex}}(1, 3) +$

$i_{23}\sigma_{\mathrm{rmin|ex}}(2,3)$, where i_{12}, i_{13}, and i_{23} are unity unless both stars in the pair are compact objects, in which case the value is zero. We apply a similar procedure to the fly-by cross section, with the cross section for clean fly-bys being given by

$$\sigma_{\mathrm{cfb}} = \sigma_{\mathrm{fb}} - \sigma_{\mathrm{rmin|fb}} \qquad (7)$$

where $\sigma_{\mathrm{rmin|fb}} = i_{12}\sigma_{\mathrm{rmin|fb}}(1,2) + i_{13}\sigma_{\mathrm{rmin|fb}}(1,3) + i_{23}\sigma_{\mathrm{rmin|fb}}(2,3)$, and, as before, i_{12}, i_{13}, and i_{23} are unity unless both stars in the pair are compact objects, in which case the value is zero.

3 RESULTS

We performed simulations of three-body encounters for three different values of q_1 and four different values of q_2, thus yielding twelve different combinations. We considered both circular and eccentric (e=0.5) binaries. In all cases the binary had a separation, $d = 60\mathrm{R}_{\odot}$, and $V_{\infty} = 10\mathrm{km/s}$. Some of these sets of encounters have been discussed elsewhere (Davies, Benz & Hills [1993, 1994]).

For each set of encounters, we computed the various cross sections as described in the previous section, and thus calculated the parameters required to obtain the cross sections for a different binary/single star encounter. These parameters are listed in Tables 1-4, the units for the masses and separations of the stars being solar, with velocities being given in units of 10km/s.

3.1 Cross Sections for Particular Binaries

We first apply the results of our three-body runs to compute the cross sections for particular binaries for a range of incoming field stars. For simplicity here, we consider only binaries containing two 0.7M$_{\odot}$ stars (*i.e.* $q_1 = 1.0$), and consider only binaries having an eccentricity, $e = 0.5$. In practice, the eccentricity of the original binaries has very little effect on the relative cross sections, rather all cross sections are increased by $\sim 50\%$ when comparing encounters involving circular binaries to those involving binaries of eccentricity, $e = 0.5$. We consider binaries of three different separations; 50R$_{\odot}$, 100R$_{\odot}$, and 200R$_{\odot}$. In the following discussion, we will assume equipartition of kinetic energy, *i.e.* $M_i V_i^2 = $ a constant. This assumption will certainly be valid in the cores of clusters, where the relaxation time is short. The mean relative speed at infinity between two stellar classes 1 and 2 can be estimated by (Verbunt & Meylan 1988)

$$\left\langle \frac{1}{V_{\infty}} \right\rangle = \sqrt{\frac{6}{\pi}\frac{1}{V_1^2 + V_2^2}} \qquad (8)$$

In Figure 1 we show the computed cross sections for mergers, clean exchanges, and clean fly-bys (shaded black, dark grey, and light grey respectively), as a function of the mass of the incoming field star, M_3. The cross sections are given in units of the clean exchange cross section obtained for the binary of separation, $d = 50\mathrm{R}_{\odot}$, with a incoming field star of mass, $M_3 = 0.7\mathrm{M}_{\odot}$. It is clear from this figure that the clean exchange cross section is a strong function of M_3; essentially no clean exchanges will occur when $M_3 \leq 0.4\mathrm{M}_{\odot}$. It should also be noted from this figure that the cross section for mergers is relatively independent of M_3. This result has been reported previously (Davies, Benz
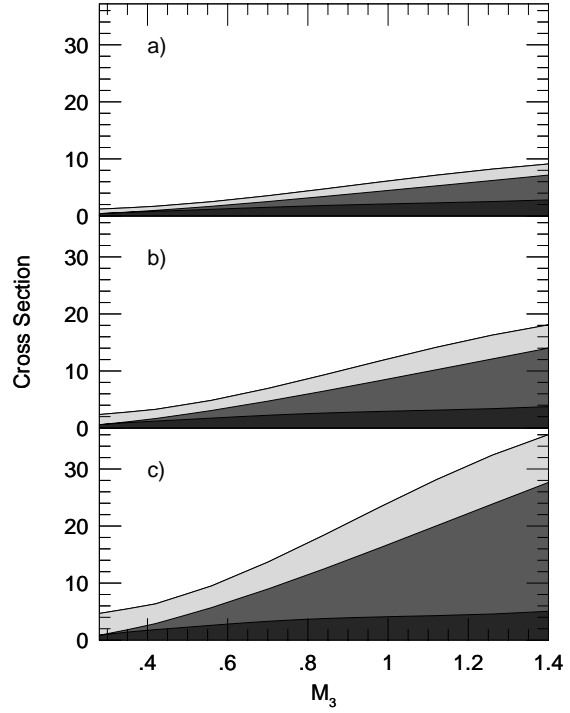

Figure 1. Relative cross sections for mergers, clean exchanges, and clean fly-bys (shaded black, dark grey, and light grey respectively) for encounters involving binaries containing two 0.7M$_{\odot}$ stars of separations a) 50R$_{\odot}$, b) 100R$_{\odot}$, and c) 200R$_{\odot}$. M_3 is given in solar units.

and Hills 1994). The total cross section for some interaction (*i.e.* $\sigma_{\mathrm{cfb}} + \sigma_{\mathrm{cx}} + \sigma_{\mathrm{rmin}}$), $\sigma_{\mathrm{tot}} \propto d$, where d is the separation of the original binary. From Figure 1, we can see that for a smaller binary separation, a lower fraction of encounters with a third star will lead to a clean exchange. As fly-bys and exchanges tend to harden a binary (by an average amount of $\sim 40\%$), one might imagine the following scenerio for the evolution of a binary fed into the core of a globular cluster: the initial binary is sufficiently wide that clean exchanges or fly-bys are more likely than mergers, however after a small number of such encounters, the binary has been hardened sufficiently that mergers are more likely. Once a merger occurs, the merged object will either be unbound to the third star, and thus the binary can be considered to have been broken up, or it will be bound to the third star, forming what we dubbed a *merged binary*. Such a binary typically has a wide separation, and thus represents a large target for subsequent encounters with other stars.

3.2 Encounter Rates for Particular Binaries

We next consider the encounter rate predicted from our computed cross sections. The rate of encounters between a given binary and the ith class of field stars, of number density, n_i, is given by $n_i \langle \sigma_{\mathrm{bi}} V_{\mathrm{bi}} \rangle$, where V_{bi} is the relative speed at infinity between the binary and the field stars of the ith class, as given in equation (8). In order to compute the encounter
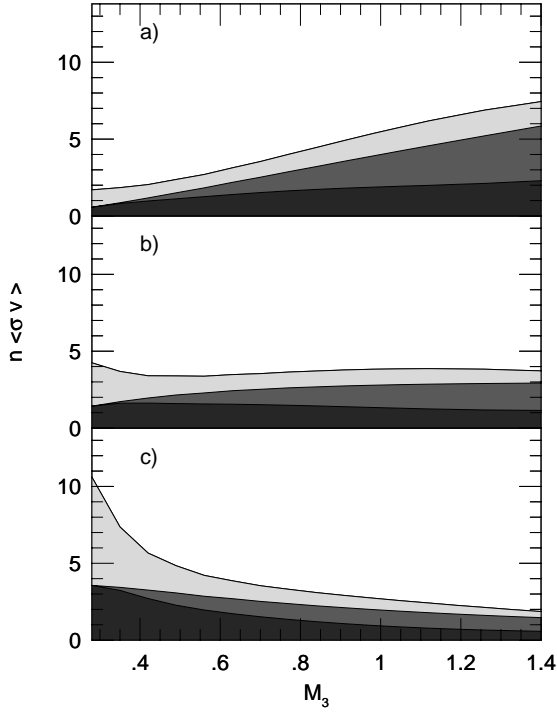
Figure 2. The relative rates for mergers, clean exchanges, and clean fly-bys (shaded black, dark grey, and light grey respectively) for encounters involving binaries containing two $0.7M_\odot$ stars of separation $50R_\odot$ for three stellar populations having values of the power law, α of a) 0, b) 1, and c) 2. M_3 is given in solar units.

Table 5. Number of stars contained in each mass bin for the three power laws considered.

mass class	M_{av}	Nature	α		
			0	1	2
1	0.1400	MS	2446.8	10000.0	24468.1
2	0.1808	MS	3160.2	10000.0	18944.8
3	0.2335	MS	4081.5	10000.0	14668.2
4	0.3016	MS	5271.5	10000.0	11357.1
5	0.3896	MS	6808.4	10000.0	8793.4
6	0.5031	MS	8793.4	10000.0	6808.4
7	0.6498	MS	5678.5	5000.0	2635.7
8	0.8393	MS	7334.1	5000.0	2040.8
9	0.6498	WD	5678.5	5000.0	2635.7
10	0.8393	WD	7334.1	5000.0	2040.8
11	1.0840	WD	18944.8	10000.0	3160.2
12	1.4000	NS	24468.1	10000.0	2446.8

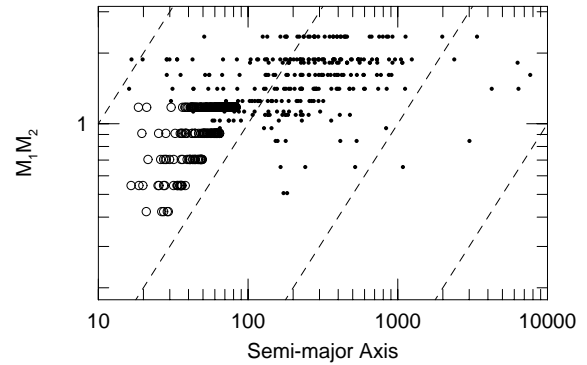The average mass for each mass bin, M_{av}, is given in solar units.

Figure 3. Clean-exchange (open circles) and merged binaries (black dots) produced in first encounters between a binary of separation, $d = 50R_\odot$, and a population having a power-law distribution with $\alpha = 0.0$ (see §4). $M_1 M_2$ is the product of the masses of the two components, given in $M_\odot$, and the semi-major axis of the binary is given in $R_\odot$.

rates as a function of field star mass, we must select a stellar population. In this general discussion, a simple power law will suffice, *i.e.* $dN/dM \propto M^{-\alpha}$. In Figure 2 we show the computed encounter rates for the binary of separation $50R_\odot$ with values of α of 0, 1, and 2, with the rates normalised to the clean exchange cross section when $M_3 = 0.7M_\odot$, and $\alpha = 0$. As in Figure 1, clean exchanges, mergers, and clean fly-bys are shaded black, dark grey, and light grey, respectively. The dependence of the relative encounter rates on α is clear; the flatter the stellar population, the greater the relative rates of clean exchanges compared to mergers. The IMF of the galaxy seems to have $\alpha \sim 2.35$, however the relatively heavy stars in a globular cluster preferentially sink to the core resulting in a flatter distribution, possibly even changing the sign of the distribution (Grabhorn *et al.* 1992).

4 PRODUCTS OF FIRST ENCOUNTERS

We now consider the products of first encounters in more detail. We consider encounters between the three different binaries and the three stellar populations considered in §3.2, leading to nine sets of runs in total. For each stellar population, we consider a total of 10^5 stars and bin them logarithmically in mass. The number of stars contained in each bin, along with the average mass of the stars in that bin, is given in Table 5, for the three values of α used. We per-

formed a monte carlo run of 10000 encounters for each of the nine combinations, counting up the number of clean exchanges, *etc* that occurred. The number of the various outcomes are listed in Table 6. From this table we see that, for a given value of α, the number of clean exchanges occurring increases with increasing binary separation, d, as expected. The majority of clean exchanges involved either a white dwarf or neutron star as the incoming third star, which is as expected; more-massive stars are more effective at removing one of the components of the original binary in an exchange. We see in all cases, the vast majority of scattering induced mergers (SIMs) involve the merger of two main-sequence stars. This is because the most common form of a SIM involves the two components of the original binary merging; here we have assumed the original binaries were comprised of two main-sequence stars. The number of merged binaries

Table 6. The frequency of the possible outcomes for first encounters between a binary and a single star, as a function of the IMF power law, α, and the separation of the binary, d.

α	d	FBs	CXs			SIMs			safe MBs			vulnerable MBs			SMOs		
			MS	WD	NS	MS	WD	NS	MS	WD	NS	MS	WD	NS	MS	WD	NS
0	50	2945	321	1204	1994	398	118	90	1456	714	620	102	19	19	12	10	3
0	100	3428	435	1497	2271	299	67	70	1005	490	413	143	41	21	6	3	0
0	200	3448	511	1696	2528	205	75	39	532	303	238	251	92	82	1	0	0
1	50	3400	411	1139	1320	442	126	57	1850	678	401	143	21	12	30	11	4
1	100	3818	557	1395	1517	320	78	40	1248	457	277	227	47	19	13	6	2
1	200	4106	580	1601	1640	238	59	27	739	264	161	348	90	47	2	0	0
2	50	4166	450	825	694	425	99	26	2342	560	199	192	15	7	33	13	1
2	100	4688	599	1029	808	343	66	13	1607	391	111	300	42	3	16	4	0
2	200	5079	727	1177	908	239	42	12	941	263	82	446	68	16	2	0	0

The initial binary was composed of two main-sequence stars of mass $0.8393 M_\odot$. CXs are clean exchanges, SIMs are scattering-induced mergers (two of the three stars merged remaining unbound to the third star), MBs are merged binaries (two of the stars merged but remain bound to the third object), and SMOs are single merged objects (all three stars merge). Merged binaries are split into safe (those resilient to being broken up by a subsequent encounter) and vulnerable (those likely to be broken up on a subsequent encounter. Each category is further subdivided by the nature of the third star the binary interacted with: MS for main-sequence stars, WD for white dwarfs, and NS for neutron stars.

produced decreases with d. We also note that the fraction of merged binaries vulnerable to being broken up by a subsequent encounter with a third star increases with increasing d. This is no surprise; it is merely that merged binaries formed from wider binaries will themselves be wider. The number of single merged objects (SMOs) is small in all cases, with more being produced for smaller values of d. Most involve three main-sequence stars, encounters between the binary and massive compact objects (*i.e.* white dwarfs and neutron stars) tend to lead to either exchanges, or merged binaries. Increasing the value of the IMF power law, α, leads to fewer neutron stars and white dwarfs, and thus the number of encounters involving such objects decreases.

In Figure 3, we plot $M_a M_b$ (where M_a and M_b are the masses of the components of the new binary) versus the semi-major axes for the clean-exchange, and merged binaries produced from encounters involving a binary of separation, $d = 50 R_\odot$, and $\alpha = 0$. Lines of constant binding energy (*i.e.* $M_a M_b / d = $ a constant) are also included. In the original binary, $M_1 M_2 \sim 0.7$, hence we can clearly see how *all* the clean-exchange binaries are harder than the original binary, with most being only slightly harder. However, a large number of the merged binaries are less bound. Other binary separations and values of α produce figures similar to Figure 3. Increasing α (*i.e.* including fewer massive stars in the population) leads, unsurprisingly, to distributions in both populations of binaries more weighted to lower values of $M_a M_b$. Larger values of d simply shifts both distributions towards greater values of semi-major axes.

In Figure 4, we plot the semi-major axis vs. eccentricity of the merged binaries and clean exchanges. Lines of constant pericentre separation are also included. From this figure, it is clear that a large fraction of post-encounter binaries will have appreciable eccentricity. We will discuss the timescale for circularisation in a later section. It is important to realise that the final separation d, after circularisation, can be considerably smaller than the initial semi-major axis of the eccentric binary, and is given by $d = (1 - e^2) d_{ecc}$. Hence if the initial eccentricity, $e \sim 0.9$, $d/d_{ecc} \sim 0.2$.
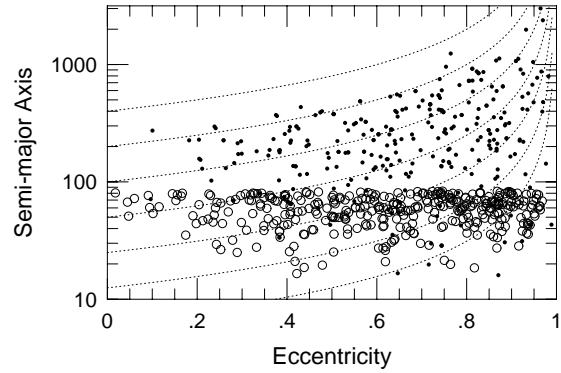

Figure 4. The semi-major axis (in solar units) and eccentricity of clean-exchange (open circles) and merged binaries (black dots) produced in first encounters between a binary of separation, $d = 50 R_\odot$, and a population having a power-law distribution with $\alpha = 0.0$ (see §4).

5 MULTIPLE ENCOUNTERS

As discussed in §4, many of the systems produced in first encounters with primordial binaries will suffer subsequent encounters in a timescale shorter than a Hubble time, in some cases in a considerably shorter time. For sufficiently wide binaries, we have seen in §4 that most encounters will result in either a fly-by, or a clean exchange. In either case, the post-encounter binary will most often have been hardened (typically by $\sim 40\%$), the change in potential energy being seen in a boost to the binary's kinetic energy. The harder the binary, the greater the kick received, of course. After only a few such encounters, the kicks are large enough to remove the binary from the core. A subsequent encounter is thus delayed until the binary has diffused back into the

Table 7. Parameters for the globular cluster models considered.

Model	α	W_0	r_0/pc	r_c/r_0	r_h/r_c	r_t/r_c	ρ_0	σ_0	$\bar{m}_c$	$M_{\rm tot}$	M_c/M_t	$\tau_{\rm rc}$	δ
A	2.00	12.0	0.73	1.22	11.14	63.40	2.E4	8	1.07	8.47E5	0.022	1.36E7	1.5
B	2.35	12.0	0.73	1.05	10.96	60.80	2.E4	8	0.93	7.70E5	0.025	1.65E7	1.5
C	2.70	12.0	0.73	0.93	11.16	59.68	2.E4	8	0.82	7.30E5	0.026	1.93E7	1.5
D	2.00	16.0	0.29	1.31	40.35	201.70	2.E5	10	1.24	2.24E6	0.005	1.93E6	2.2
E	2.35	16.0	0.29	1.20	32.70	163.54	2.E5	10	1.10	1.76E6	0.007	2.30E6	2.1
F	2.70	16.0	0.29	1.06	33.56	163.71	2.E5	10	0.96	1.65E6	0.007	2.66E6	2.1
G	2.35	8.0	1.74	0.88	3.97	20.95	2.E3	6	0.76	3.00E5	0.084	1.08E8	1.0
H	2.35	6.0	2.32	0.81	2.74	12.60	5.E2	4	0.67	1.00E5	0.147	1.65E8	0.9
I	2.35	4.0	2.75	0.72	2.05	7.79	2.E2	3	0.58	3.37E4	0.270	2.21E8	0.6

α is the exponent of the IMF power law, W_0 is the depth of the potential well (in unit of the central velocity dispersion σ_0). r_0 is the characteristic radius (in pc), r_c is the core radius, r_h is the half-mass radius, and r_t is the tidal radius. The central density, ρ_0, is given in units of $\mathrm{M}_\odot/\mathrm{pc}^3$. The central velocity dispersion of stars of mass $\bar{m}_c$ (given in $\mathrm{M}_\odot$), σ_0 is given in km/s. The total mass of the cluster, M_t is given in $\mathrm{M}_\odot$. M_c is the mass of the cluster core. The core relaxation timescale, $\tau_{\rm rc}$, is given in years. δ is the parameter fit for the gravitational potential (see equation [22]).

core again, this time being a very sensitive function of the apogee of the trajectory of the binary.

When discussing energetics of stars in globular clusters, it is convenient to work in units of $m\sigma^2 = kT$, where m is the mean mass of stars in the core, and σ is the characteristic 1-D velocity dispersion. For single-mass models of moderately concentrated clusters, the central potential $\sim 5 - 10kT$ (Binney & Tremaine 1987). For stars of equal mass, the third star carries off $2/3$ of kinetic energy in the recoil, hence to eject the binary from the cluster we require $\Delta E \sim 30 - 60kT$ (as the binary contains two stars). Given that a binary typically hardens by about 40%, binaries are therefore vulnerable to ejection once they harden to $E_{\rm bin} \sim 80 - 160kT$. The equivalent binary separation will depend on the velocity dispersion, and the masses of the components, but assuming $\sigma \sim 10$km/s, and stars of solar mass, yields a separation of $d \sim 20 - 40 \mathrm{R}_\odot$.

5.1 Cluster Models

We use King-Mitchie models to describe various globular clusters. We model the stellar population by some power law, where the number of stars having a mass between m and $m + dm$ is given by $dN(m) \propto m^{-\alpha} dm$. The stars are binned by mass into different classes j and the stellar distributions are computed using a distribution function having a lowered Maxwellian energy dependence (King 1966), with an anisotropy term taking the form $\exp(-\beta J^2)$ (Mitchie 1962). For the jth mass bin, we have

$$f_j(E, J) \propto (e^{-A_j E} - 1)e^{-\beta J^2} \qquad (9)$$

For details of the calculation of King-Mitchie models, see Gunn and Griffin (1979). The problem reduces to the solution of a first order system

$$\xi^2 \frac{dW}{d\xi} = -U, \quad \frac{1}{\xi^2}\frac{dU}{d\xi} = 9\tilde{\rho}(\xi, W) \qquad (10)$$

where $\xi = r/r_0$, $W = \psi/\sigma^2$, $\tilde{\rho} = \rho/\rho_0$ and $U = 9\int_0^\xi \sigma\xi'^2 d\xi'$; r_0 being the scale radius, σ is the velocity dispersion of stars of mass, $\bar{m}_c$ ($\bar{m}_c = \tilde{\rho}_0^{-1}\sum m_j\tilde{\rho}_j$). The central velocity dispersion is denoted σ_0 and ρ_0 is the central density. The

normalised density at a given radius, $\tilde{\rho}(\xi, W) = \sum \tilde{\rho}_j(\xi)$, where the density contribution of each mass class of stars, $\tilde{\rho}_j(\xi) = \alpha_j I_1(\mu_j W, \xi/\xi_a)/I_1(\mu_j W_0, 0)$ where $\xi_a = r_a/r_0$, r_a being the *anisotropy* radius, $\mu_j = m_j/\bar{m}$, and $I_1(x, y) = \int_{|u|<(2x)^{1/2}} \exp(-\frac{1}{2}y^2 u_\perp^2) \times [\exp(-\frac{1}{2}u^2 + x) - 1]d^3u$. α_j is thus the contribution to the central density from mass bin j. In the models we consider here, we simplify the models by assuming the velocity dispersion is iostropic for the whole of a cluster (i.e. $r_a = \infty$). In a companion work (Davies & Benz [1994]), we consider models for the globular clusters for ω Cen and 47 Tuc produced by Meylan (1987, 1989) which include a non-trivial anisotropy radius.

The value of the scale radius, r_0, is given by

$$r_0 = \sqrt{\frac{9\sigma_0^2}{4\pi G\rho_0}} \qquad (11)$$

The total mass of the system, $M_{\rm tot}$ is given by

$$M_{\rm tot} = \left(\frac{r_0\sigma_0^2}{G}\right) U_{\rm tot} \qquad (12)$$

where $U_{\rm tot} = 9\int_0^{\xi_t} \sigma\xi'^2 d\xi'$.

With W_0, ξ_a, and α_j for all the mass bins specified, equation (10) can be integrated until $W = 0$ at which point we have reached the cluster edge. One adjusts the values of α_j until the fractions of mass contained in the various mass bins agrees with the assumed mass function. Thus we are able to compute the density of each mass bin as a function of radius given certain characteristics of the globular cluster.

A choice of σ_0^2 and ρ_0 then yield a physical value for r_0, and $M_{\rm tot}$. It should be noted that r_0 *and the core radius,* r_c *are not necessarily identical.* The core radius is defined *observationally* as the radius at which the surface brightness is half the central value. The scale radius takes its definition from equation (11) and is the core radius for stars of mass $\bar{m}_c$. The two radii will take different values as long as the turn-off mass (the mass of the stars contributing mostly to the surface brightness) differs from $\bar{m}_c$. The difference is computed here, though the discrepancy is relatively small, always being less than 30%.

Table 8. Number of stars contained in each mass bin for the cores of the nine globular cluster models.

mass class	M_{av}	Nature	A	B	C	D	Model E	F	G	H	I
1	0.1400	MS	900	1872	3239	86	234	416	8628	7757	6736
2	0.1808	MS	787	1528	2489	78	198	334	6673	5826	4905
3	0.2335	MS	720	1327	2037	76	183	296	5327	4498	3666
4	0.3016	MS	711	1245	1844	81	189	303	4472	3542	2729
5	0.3896	MS	778	1330	1929	101	232	378	4013	2938	2104
6	0.5031	MS	992	1686	2438	155	363	621	3952	2572	1670
7	0.6498	MS	1549	2632	3732	320	776	1405	4356	2428	1370
8	0.8393	MS	3044	4873	6164	949	2286	4006	5278	2473	1185
9	0.6498	WD	1797	2420	2736	371	714	1030	4005	2232	1260
10	0.8393	WD	2098	2422	2222	654	1136	1445	2623	1229	589
11	1.0840	WD	4602	3934	2597	2610	3365	2964	2881	1167	478
12	1.4000	NS	4259	1929	724	4890	2699	1158	1110	414	153
total			22237	27198	32152	10372	12376	14357	53320	37074	26846
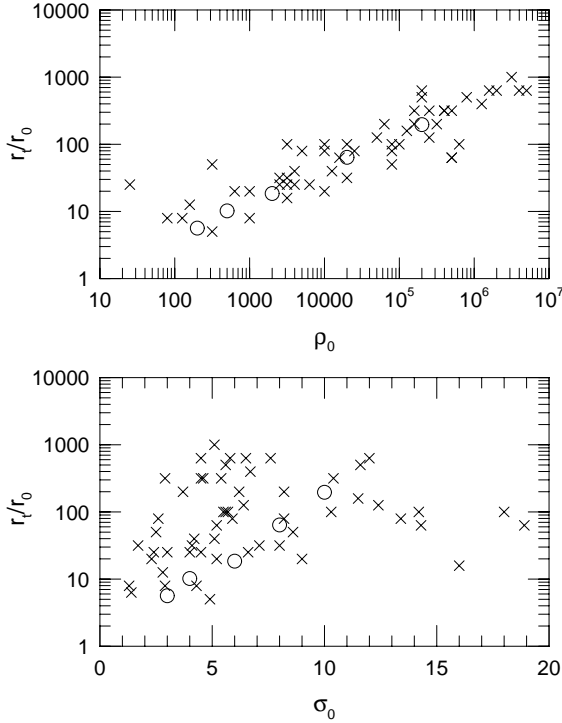
Figure 5. The tidal radius divided by the scale radius, r_t/r_0, as a function of a) ρ_0 and b) σ_0 for the 56 clusters modelled by Pryor & Meylan (1993), labelled with "×"s and for our cluster models with $\alpha = 2.35$ (labelled with open circles).

We considered three power laws for the IMF, taking values of α of 2.00, 2.35, and 2.70. We considered stars having a mass between $0.14 M_\odot$ and $15.0 M_\odot$. Stars more massive than $8.0 M_\odot$ were considered to evolve into neutron stars via type II SN. Those between 4.7 and $8.0 M_\odot$ are deemed to leave no remnant (Iben & Renzini 1983), whilst the remaining stars above the present turn-off leave white dwarfs of mass, $M_{wd} = 0.58 + 0.22(M_{ms} - 1) M_\odot$. The stars are then binned in the same manner as the populations listed in Table 5.

We considered values of the central potential depth, W_0, ranging from 4 to 16. For a given IMF, we solved equation (10) to produce the spatial distribution of the stars in each mass class. Suitable values for σ and ρ_0 were then chosen by comparing our model clusters with properties derived for 56 clusters by Pryor & Meylan (1993). In Figure 5 we plot the concentration, r_t/r_0, as a function of ρ_0 and σ for the 56 clusters studied by Pryor & Meylan. The values adopted for our models for $\alpha = 2.35$ are also shown (r_t/r_0 was found to be largely independent of α for the range of IMFs we considered). Having selected values for ρ_0 and σ, the values for r_0 and M_{tot} were computed, and are listed in Table 7, together with other properties of the globular cluster models.

To obtain the total stellar population in the core, we integrated the number densities of the various stellar species out to a scale radius. The stellar population in the core of a cluster differs from the IMF of the whole cluster; mass segregation results in the core containing more massive stars. This effect is more pronounced in more collapsed clusters (i.e. clusters with a larger value of W_0), as can be seen in Table 8.

5.2 Encounters between Two Single Stars

Before we consider encounters between binaries and single stars, we consider the rate of encounters between two single stars, given the core models in Table 8. The rate of encounters between two stellar species, 1 and 2, passing within some minimum distance, R_{min} is given by

$$\Gamma_{12} = 6 \times 10^{-9} \frac{n_1}{10^4 \text{ pc}^{-3}} \frac{n_2}{10^4 \text{ pc}^{-3}} \frac{M_1 + M_2}{\text{M}_\odot}$$
$$\times \frac{R_{min}}{\text{R}_\odot} \frac{10 \text{kms}^{-1}}{V_\infty} \text{ yr}^{-1} \text{pc}^{-3} \qquad (13)$$

where n_1 and n_2 are the number densities of the two species. We use an analytic expression for R_{min} suggested by Benz and Hills (1991):

$$\frac{R_{min}}{R_1} = 3.28 + 0.45 \log\left(\frac{M_2}{M_1}\right) + 0.22 \log\left(\frac{M_1}{\text{M}_\odot} \cdot \frac{\text{R}_\odot}{R_1}\right) \quad (14)$$

Table 9. The production rates of blue stragglers (BS), white dwarf/main-sequence star (WD-MS), and neutron star/main-sequence star (NS-MS) systems via encounters between single stars in various globular cluster models.

Model	W_0	α	BS	WD-MS	NS-MS
A	12.0	2.00	0.372	0.931	0.666
B	12.0	2.35	1.124	1.656	0.537
C	12.0	2.70	2.264	1.970	0.291
D	16.0	2.00	0.242	1.250	2.260
E	16.0	2.35	1.489	4.489	3.186
F	16.0	2.70	4.876	8.521	2.566
G	8.0	2.35	0.230	0.272	0.096
H	6.0	2.35	0.123	0.062	0.009
I	4.0	2.35	0.047	0.017	0.002

Encounter rates are given in units of encents per 10^8. W_0 is the depth of the cluster potential well (in units of the central velocity dispersion), and α is the exponent of the IMF power law.

We thus calculate the encounter rates between the various stellar species for the models listed in Table 8; the results being listed in Table 9, with production rates being given in units of encounters/10^8 years. We assume here that all close encounters between two main-sequence stars that become bound produce blue stragglers. There has been much debate concerning whether binaries can be formed via tidal capture. Here we simply list all close encounters between main-sequence stars and white dwarfs and neutron stars. Some fraction of these encounters may lead to binaries rather than a smothered compact object. Simulations suggest that less than half the encounters produce binaries (Davies, Benz & Hills 1992). From Table 8, we see that the encounter rates are an extremely strong function of cluster concentration. The most-collapsed clusters (models D, E, and F) show larger rates. The rates are also seen to be a function of the IMF; smaller values of the power-law exponent, α, implies a larger fraction of neutron stars and white dwarfs compared to main-sequence stars, and this difference is echoed in the encounter rates.

5.3 Timescales

The components of a tight binary will spiral-in because of angular momentum losses via magnetic winds and gravitational radiation. For the binaries containing at least one main-sequence, it has been suggested that magnetic breaking will dominate over general relativistic effects (Verbunt & Zwaan 1981). The timescale for two stars to spiral-in from a distance $d_{\rm init}$ to a separation $d_{\rm final}$ is given by (DiStefano & Rappaport 1992)

$$
\tau_{\rm mb} = 4.3 \times 10^5 \left(\frac{M_2}{M_\odot} \right) \left(\frac{R_\odot}{R_1} \right)^\gamma \left(\frac{M_\odot}{M_1 + M_2} \right)^2
$$
$$
\times (d_{\rm init}^4 - d_{\rm final}^4) \ \text{years} \tag{15}
$$

where here we will take $\gamma = 1$.

For systems containing two compact objects, inspiral will still occur due to angular momentum loss from gravitational radiation. Beginning from a separation d, merger will occur on a timescale given by (Landau & Lifshitz 1962)

$$
\tau_{\rm gr} = 1.55 \times 10^8 \left(\frac{M_1}{M_\odot} \right)^{-1} \left(\frac{M_2}{M_\odot} \right)^{-1} \left(\frac{M_1 + M_2}{M_\odot} \right)^{-1}
$$
$$
\times \left(\frac{d}{R_\odot} \right)^4 \ \text{years} \tag{16}
$$

For binaries, of separation d, containing a convective star of mass M_1 and radius R_1, and a compact object of mass M_2, the timescale for the circularisation of the binary is given by (DiStefano & Rappaport 1992)

$$
\tau_{\rm circ} = 2.7 \left(\frac{M_1}{M_2} \right) \left(\frac{M_1}{M_1 + M_2} \right) \left(\frac{d}{R_1} \right)^8 \ \text{years} \tag{17}
$$

If a binary circularizes, the final separation, $d = (1 - e^2)d_{ecc}$ where d_{ecc} is the semi-major axis of the eccentric binary, having eccentricity, e.

The timescale for a binary of separation d to encounter something is largely independent of the slope of the IMF (see Figure 2). It can be approximated by

$$
\tau_{\rm enc} \sim 3 \times 10^{11} \frac{1}{n_4} \left(\frac{d}{R_\odot} \right)^{-1} \ \text{years} \tag{18}
$$

where n_4 is the total number density of stars in units of $10^4/{\rm pc}^3$.

For computational simplicity, the gravitational potential for one of the globular cluster models can be approximated (for $r_c < r < 10^\delta r_c$) as

$$
\Phi \sim \frac{\Phi_0}{\delta} \log \left(\frac{r}{r_c} \right) - \Phi_0 \tag{19}
$$

where Φ_0 is the depth of the potential. δ was determined empirically for each model, and is listed in Table 7.

The relaxation time can be taken to be $\tau_r = \tau_{\rm rc}(r/r_c)^2$ where the core relaxation time, $\tau_{\rm rc}$ is given by (Lightman & Shapiro 1977)

$$
\tau_{\rm rc} = 1.55 \times 10^7 \frac{(M_\odot/m)}{\log(0.5 M_t/m)} \left(\frac{\sigma}{km/s} \right) \left(\frac{r_c}{pc} \right)^2 \tag{20}
$$

where m is the mean stellar mass in the core, and M_t is the total mass of the cluster, as listed in Table 7.

Using the assumptions discussed above for the potential well of a globular cluster and the radial dependence of the local relaxation time, we can compute the timescale for the return of a binary to the core of a cluster, having been removed with specific energy $\epsilon_{\rm kick}$. Following Hut, McMillan & Romani (1992), we assume the evolution of the orbital apocenter, r_a, is given by

$$
\frac{1}{r_a} \frac{dr_a}{dt} = \frac{1}{\tau_r(r_{\rm eff})} \tag{21}
$$

where $r_{\rm eff} = (r_c^3 r_a)^{1/4}$, and τ_r is the local relaxation time. Intergration and simple algebra then gives the timescale for return to the core as

$$
\tau_{\rm ret} \sim \frac{2}{3} \tau_{\rm rc} \left(10^{(3\delta \epsilon_{\rm kick}/2\Phi_0)} - 1 \right) \tag{22}
$$

These various timescales are plotted in Figure 6, for three different cluster models. For simplicity here we assumed all stars were solar. In all three plots, the timescales for inspiral via magnetic winds and gravitational radiation are unchanged, as is the timescale for binary circularisation,

as these depend purely on the properties of the binary, of-course. Both the encounter timescale and the timescale to return to the core, assuming the binary received a kick in its last encounter, increase with decreasing density. For a binary of separation, $d = 1000R_\odot$, the encounter timescale ranges from $\sim 10^7$ years for the densest cluster shown in Figure 6, to $\sim 10^9$ years for the least dense. As we shall see later, this range in timescales will turn out to be crucial in determining what fraction of binaries will have suffered many encounters in a cluster core, leading often to ejection, merging, or breakup. Imagine that we begin with a binary of separation, $d = 1000R_\odot$. From Figure 6, we note that in the densest two cluster cores, the binary will quickly encounter a third star. In such wide binaries, most encounters will ei-ther be a fly-by or a clean exchange. In either outcome, we will be left with a detached, but hardened, binary. Typi-cally, we expect the binary to be hardened by 40%, in other words we expect $d_{new} \simeq 0.7d_{old}$. As for the two densest clus-ters, $\tau_{enc} \ll 10^{10}$ years, we expect this binary to undergo many subsequent encounters, gradually getting harder. As the binary gets harder, encounters with a third star are more likely to lead to a merger. We have seen that merged binaries tend to have much larger separations, hence we expect any merged binaries to rapidly undergo a subsequent encounter (on a timescale $\sim 10^7 - 10^8$ years for the two densest clus-ters considered in Figure 6). We note from Figure 6a that $\tau_{enc} \sim 10^{10}$ years when $d \sim 100R_\odot$. We are therefore un-likely to produce many binaries much harder than this in such low-density clusters, and in turn we expect the number of merged systems to be reduced.

It is also important to note that $\tau_{ret} \ll \tau_{enc}$ for $d \geq 10 - 20R_\odot$. τ_{ret} increases rapidly with decreasing d for $d \sim 10 - 20R_\odot$, as binaries of this separation will get ejected from the core almost to the outer edge of the cluster halo, and thus take an extremely long time to diffuse back into the core. It is also worth noting that in the three clusters considered in Figure 6, subsequent encounters on timescales $\leq 10^{10}$ years are not delayed significantly by having to wait for the binary to re-enter the core.

We see from Figure 6 that magnetic breaking will bring a $1M_\odot$ main-sequence star and its $1M_\odot$ companion to-gether in $\leq 10^{10}$ years, if $d \leq 10R_\odot$. Gravitational radia-tion performs a similar function when the initial separation $d \leq 4R_\odot$. In order to reach such small initial separations, we will first have to pass through a common envelope phase, as will be discussed in the next section.

We note also that $\tau_{circ} \leq 10^{10}$ years for $d \leq 20R_\odot$. Recalling that after circularisation, $d = (1 - e^2)d_{ecc}$, we see that relatively wide, eccentric binaries, ultimately evolve into much smaller, circular, ones. For example, a binary with $e = 0.8$, and $d_{ecc} = 30R_\odot$ will produce a circular binary, with $d \simeq 10R_\odot$. In other words, if we can produce fairly hard bi-naries ($d \sim 10 - 40R_\odot$) with sizeable eccentricity, these may then circularise into systems hard enough to come into con-tact in a Hubble time.

5.4 Stellar Evolution Issues

A white dwarf smothered by the remnant of a main-sequence star will evolve into a red giant on a thermal timescale ($10^6 - 10^7$ years). Such objects contained in resilient merged binaries will engulf the other component of the binary form-
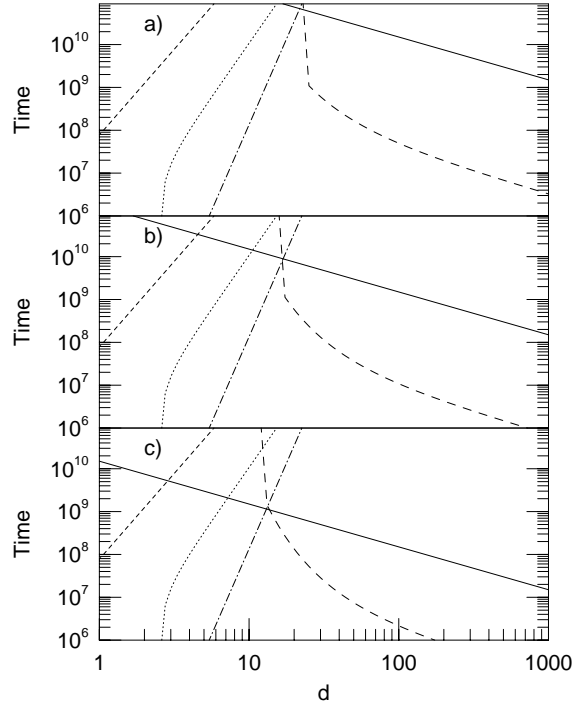

Figure 6. The various timescales (in years) for the cores of three globular cluster models as a function of the binary separation, d (given in solar units). The three models have different central den-sities: a) $2000M_\odot/pc^3$, b) $2 \times 10^4 M_\odot/pc^3$, and c) $2 \times 10^5 M_\odot/pc^3$. The timescale for an encounter with a single star is shown with a solid line, the timescale to return to the core after being ejected by an encounter is given with a long-dashed line. The timescale for circularisation is given by a dot-dashed line, whilst the timescales for inspiral due to magnetic breaking and gravitational radiation are given by dotted and short-dashed lines respectively.

ing a common envelope system. In such a system, the white dwarf and other component will spiral together as the com-mon gaseous envelope is ejected. The final separation of the two stars may be estimated by simply equating the binding energy of the envelope with the change in binding energy of the two stars, within some efficiency α_{ce}. We thus have

$$E_{env} = \alpha_{ce}\Delta E_g$$
$$\text{where } E_{env} = \frac{G(M_c + M_e)M_e}{\lambda a_i r_l}$$
$$\text{and } \Delta E_g = \frac{GM_2 M_c}{2a_f} - \frac{GM_2(M_e + M_c)}{2a_i} \quad (23)$$

Where M_e and M_c are the envelope and core masses, M_2 is the mass of the second star, a_i and a_f are the initial and final separations, r_l is the Roche lobe radius of the red giant, and λ depends on the structure of the red giant envelope and ~ 0.5. Hence with a choice of α_{ce} (typically taken to be 0.2-0.4 [Taam & Bodenheimer 1989]), we are able to compute the final separation of the white dwarf and second star. Such a mechanism will be of great use in producing hard binaries in globular clusters.

Next we consider neutron stars smothered by main-sequence stars. The subsequent evolution of such an object is extremely uncertain. It is possible that a stable envelope configuration can be obtained where material is accreted onto the surface of the neutron star and supports the envelope. Such a *Thorne-Zytkow Object* will live for $\sim 10^6$ years as a supergiant before the envelope has been completely ejected via a wind (Cannon 1993). If we assume this evolutionary scenario is correct, then any smothered neutron stars contained in binaries will lead to common envelopes as the envelope expands. The evolution can then be modelled as described above for smothered white dwarfs. It has also been suggested that the envelope will be ejected after an extremely small amount of material has been accreted. If this latter scenerio is correct, then no common envelope phase will occur, and the merged binaries are likely to broken up by the instantaneous mass loss, or the binaries will be so weakly bound after the episode of mass loss that they are likely to be broken up by an encounter with a passing third star.

5.5 The Evolution of Binaries in Globular Cluster Cores

Following Hut, McMillan & Romani (1992), we consider the core of a globular cluster to be composed of a static population of single stars and a population of evolving binaries. In practice, the background of single stars will also be evolving, though the core may be supported from collapse by the energy released from the binaries. This analysis represents a reasonable intermediate step until a full n-body treatment is conducted. We imagine binaries diffusing into the core, encountering a single star (or perhaps many single stars) and producing some new binary/object. We neglect 2+1 encounters occuring outside of the core (this is not unreasonable as only a small fraction of the encounters will occur outside of the core). For a given binary, we compute its cross sections for interactions with all the different mass classes of single stars, select one at random (weighted by the cross sections) thus producing a new object. If the new system is a binary that is not ejected from the cluster, we repeat the process, thus simulating subsequent encounters. If the new binary is removed from the core, but not from the cluster, we estimate a timescale for the binary to return to the core, as given by equation (22), and reinsert it into the core after the computed delay.

We injected 1000 binaries into the core of each of the cluster models and evolved the binaries until one of the following occurred: 1) a merged object was produced in a scattering-induced merger (SIM), 2) the binary was deemed to be likely to be broken up through an encounter with a third star ($M_1 M_2/d < 0.001$ in solar units), 3) a single merged object (SMO) was produced, 4) the binary was ejected from the cluster, or 5) the binary was deemed to have come into contact via inspiral from either a magnetized wind or gravitational radiation. Additionally, in some runs we halted the evolution of the binaries when a smothered neutron star was produced, as the subsequent evolution of such an object is currently unclear.

There are clearly a great number of parameters we can vary; the cluster model, described by its IMF, and concentration, the population of binaries we feed into the cluster
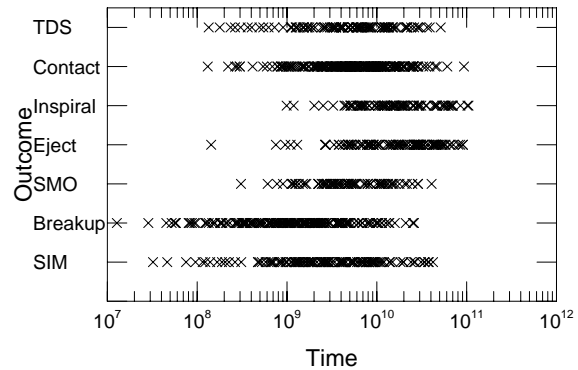

Figure 7. Final outcome of the binaries evolved in Run 1, as a function of when the final object was produced. SIM are scattering-induced mergers, SMOs are single merged objects, TDS refers to smothered neutron stars (thick disk systmes). Contact refers to binaries brought together via magnetic breaking, whilst inspiral refers to binaries brought together via gravitational radiation.

core, and their distribution of injection times. We also have to decide how long to evolve the cluster binaries for. Finally, we have to consider two stellar evolution issues; assigning a value to the efficiency of the common envelope phase, α_{ce}, and deciding how to treat smothered neutron stars (see §5.4). Rather than consider the full range of possibilities here, we show a restricted set, changing only one of the above parameters at a time in an attempt to show trends.

5.6 The Effect of Changing the Injection Time and Duration of the Run

We will begin by considering a moderately concentrated cluster ($W_0 = 12.0$) with an IMF, $\alpha = 2.35$. In run 1, we injected 1000 binaries (each containing two $0.8393 M_\odot$ main-sequence stars) into the core and let them evolve until one of the criteria described above were met. The initial binary separations were chosen randomly with equal probability in $\log d$ from the range $100 R_\odot < d < 704 R_\odot$ (the upper being by forcing $M_1 M_2/d > 0.001$ in solar units; this being the criteria for a hard binary unlikely to be broken up by a passing third star). In this run, we stop the evolution of a binary as soon as a smothered neutron star is produced, labelling the outcome as a TDS. We also adopted $\alpha_{ce} = 0.4$. In Figure 7 we plot the final outcomes of the 1000 binaries as a function of when the outcomes occurred. The first thing to note from this plot is that a fraction of the binaries are not resolved until much later than 15Gyr after they have been inserted into the cluster core. We see from Figure 7 that breakup and SIM events occur almost immediately with a large fraction of such events occurring after a few Gyr. However, we see that ejection and binary coalescence events (labelled as contact and inspiral in the figure) tend to occur later. This is not surpising; in the case

Table 10. The outcomes of the evolution of 1000 binaries in various cluster models.

Run	W_0	α	α_{ce}	BP	t_{evol}	t_{inj}	BS	TDS	contact binaries						MGRI		
									XB	CV	SN	SW	BS	NW	WD_a^2	WD_b^2	NS^2
1	12.0	2.35	0.4	A	∞	0.0	343	157	44	77	5	54	93	33	51	1	–
2	12.0	2.35	0.4	A	15.0	0.0	365	121	16	69	2	53	76	21	30	0	–
3	12.0	2.35	0.4	A	15.0	15.0	295	86	16	32	4	42	34	5	11	0	–
4	12.0	2.35	0.4	B	15.0	15.0	191	66	9	32	1	17	48	11	8	0	–
5	12.0	2.70	0.4	B	15.0	15.0	305	34	10	38	1	32	50	2	6	0	–
6	12.0	2.00	0.4	B	15.0	15.0	107	105	22	20	0	15	25	5	11	0	–
7	12.0	2.35	0.4	B	15.0	15.0	188	–	22	33	0	14	52	10	11	0	1
8	12.0	2.35	0.4	A	15.0	15.0	273	–	22	30	5	42	56	14	15	0	0
9	12.0	2.35	0.4	A	∞	15.0	361	–	63	86	12	75	73	77	54	1	16
10	12.0	2.35	0.4	B	∞	15.0	272	–	52	85	4	58	79	74	57	0	18
11	12.0	2.35	0.2	B	15.0	15.0	186	–	9	31	0	21	44	17	10	0	5
12	12.0	2.35	0.1	B	15.0	15.0	185	–	16	24	1	17	42	18	32	0	4
13	12.0	2.35	0.05	B	15.0	15.0	178	–	17	24	2	11	39	31	35	0	7
14	16.0	2.35	0.05	B	15.0	15.0	168	–	24	31	2	9	19	138	42	0	66
15	16.0	2.35	0.4	B	15.0	15.0	144	–	47	37	0	7	23	86	31	0	28
16	16.0	2.35	0.4	B	15.0	15.0	169	220	22	29	0	9	29	34	29	0	–
17	16.0	2.35	0.4	B	15.0	0.0	150	287	21	34	0	9	30	39	28	0	–
18	16.0	2.00	0.4	B	15.0	15.0	86	223	27	12	1	2	8	19	9	0	–
19	16.0	2.70	0.4	B	15.0	15.0	280	160	13	49	4	33	54	35	55	0	–
20	16.0	2.00	0.4	B	15.0	15.0	83	–	39	13	0	1	16	40	3	0	41
21	8.0	2.35	0.4	B	15.0	15.0	65	2	1	2	1	7	19	0	0	0	0
22	6.0	2.35	0.4	B	15.0	15.0	31	0	0	0	0	0	10	0	0	0	0
23	4.0	2.35	0.4	B	15.0	15.0	13	0	0	1	0	0	2	0	0	0	0

W_0 is the depth of the cluster potential (in units of the central velocity dispersion). α is the exponent of the power-law IMF. α_{ce} is the efficiency in the common envelope stage. BP is the binary population: in type A, the initial binaries always contain two $0.8393 M_\odot$ main-sequence stars, in type B they contain two main-sequence stars drawn independently from the IMF, with the extra criterian that their total mass $> 1 M_\odot$. t_{evol} is the total time the binaries were allowed to evolve (in Gyr), with the binaries being initially injected into the core at a time drawn randomly between zero and t_{inj}, given in (Gyr). BS is the number of blue stragglers produced when two main-sequence stars collided during an encounter.

TDS is the number of smothered neutron stars produced (when this was one of the criteria for terminating the evolution of the binary). Contact binaries are those systems brought into contact via angular momentum loss by magnetic winds. This outcome is further subdivided into: X-ray binaries (XB) when the system contains a neutron star more massive then its main-sequence companion, cataclysmic variables (CV) when the system contains a white dwarf more massive than its main-sequence companion, smothered neutron stars (SN) and smothered white dwarfs (SW) when the compact objects are less massive than their companions, and blue stragglers (BS) when both components are main-sequence stars. Systems brought into contact via gravitational radiation are labelled MGRI (mergers through gravitational radiation inspiral). This outcome is further subdivided into: neutron star/white dwarf mergers (NW), white dwarf/white dwarf mergers (WD^2), and neutron star/neutron star mergers (NS^2). WD^2 are further subdivided into those where the total mass exceeds the Chandrasekhar mass (WD_a^2) and those of smaller total mass (WD_b^2).

of ejections, the binary must first harden via exchanges and fly-bys until the recoil is sufficient to remove it from the cluster. To produce a coalescence via inspiral from gravitational radiation (labelled simply as inspiral in the figure), the binary first passes through a CE phase, the two compact objects being left $\sim 3R_\odot$ apart. These two stars then spiral together as angular momentum is lost through gravitational radiation on a timescale ~ 10Gyr. Binaries may also be brought into contact as angular momentum is lost via a magnetized wind from a main-sequence star component of the binary, on a timescale $\sim 1 - 5$Gyr, if the initial separation $\sim 8R_\odot$. Single-merged objects (SMOs) are produced only for encounters involving hardened binaries hence are only seen after $\sim 1 - 10$Gyr.

In Table 10 we list the frequencies of the various possible outcomes. For the systems brought into contact by angular momentum loss from a magnetized wind we differentiate between five possible outcomes: if a main-sequence star is filling its roche lobe and transferring material to a neutron star an LMXB will be produced if the neutron star is the more massive of the two stars, otherwise a thick-disk system (TDS) will be produced with the neutron star smothered by the remains of the main-sequence star; we apply a similiar criterion for mass transfer onto a white dwarf, producing either a CV if the white dwarf is more massive, or a smothered white dwarf. This approximation is reasonable given the nature of these simulations. Finally, if both components of the binary are main-sequence stars, we tag the merged object as a blue straggler. This is another mechanism for producing blue stragglers in addition to those produced di-

rectly through collisions of two main-sequence stars during a 2+1 encounter.

For systems coalescing after losing angular momentum via gravitational radiation, we distinguish between the following outcomes: the system may contain two neutron stars, a neutron star and a white dwarf, or two white dwarfs. In the latter case, we further distinguish between those systems containing a total mass greater than the Chandrasekhar limit ($1.4M_\odot$) and those less massive.

Run 2 is identical to run 1 except that we only evolved the binaries for 15 Gyr. Of the 1000 binaries, 212 of them were unresolved at the end of the run (in other words, they had not reached some end state, such as merging or ejection). In run 3, we injected the binaries at some random time drawn evenly between zero and 15 Gyr, and evolved them up to a time of 15 Gyr. This procedure increased the number of unresolved systems to 474. In other words, in a fairly concentrated cluster, a large fraction of the binaries that have entered the core will still be present today.

In runs 1-3, the number of smothered neutron stars produced greatly exceeds the number of LMXBs produced, by a factor $\sim$ 5. Also, the number of white dwarf/white dwarf merger events produced via gravitational-radiation inspiral is approximately comparable to the production rate of LMXBs. One might therefore be optimistic that a large fraction of the MSPs observed in globular clusters may have been produced through evolutionary paths not including an LMXB phase, for example by accretion from the thick disk surrounding the neutron star in smothered systems (Krolik 1984). It should also be noted that the fate of a white dwarf/white dwarf merger is unclear; such an event may produce a supernova leaving no remnant, or the neutron produced may not have a low magnetic field or rotate rapidly (Phinney & Kulkarni 1994).

All three runs produced $\sim$ 300-400 blue stragglers.

Limiting the evolution time, and inserting the binaries at random times rather than at a time of zero both reduced the production of contact binaries and mergers via GR inspiral. From Table 10 we see that the number of LMXBs and CVs produced decreases from 121 to 48 comparing run 1 to run 3. We believe globular clusters are $\sim$ 15 Gyr old, and a steady flow of binaries into the core may be more physical than an instantaneous insertion of all of them at zero age. Hence, one might believe run 3 to be the physically more relevant of runs 1-3.

5.7 The Effect of Changing the IMF

In the first three runs, we considered the binary to be comprised of two $0.8393M_\odot$ main-sequence stars. The actual binaries are more likely to be composed of stars having a range of masses, hence we now allow the binaries to be composed of stars of different mass, drawing the masses of the two stars independently from the IMF, with the additional criterion that the total mass be larger than $1M_\odot$, this being typical of the average mass of stars in the cores of fairly concentrated clusters. In runs 4-6, we evolve the binaries for 15 Gyr, and inject them at random times as was done in run 3. We consider three values for the IMF, α having values of 2.35, 2.70, and 2.00 for runs 4, 5, and 6, respectively (where the IMF is given by the power law, $dN/dm \propto m^{-\alpha}$). The number of blue stragglers produced is seen to be a sensitive function

of the IMF; fewer blue stragglers are produced for smaller values of α. The number of smothered neutron stars also depends on α. The flatter the IMF, the larger the number of neutron stars in the core, and thus the production rate of TZOs and LMXBs increases, whilst the production of CVs becomes less likely. This effect has already been noted by Hut & Verbunt (1984).

5.8 The Effect of the Evolution of Smothered Neutron Stars

We now consider the effect of assuming a smothered neutron star in a binary will expand to form a red giant and engulf its companion forming a CE phase, in a manner analogous to that for smothered white dwarfs, rather than evolve rapidly to some cataclysmic event such as a supernova explosion. In runs 7-10, we injected 1000 binaries at randon times into the core of the cluster having $W_0 = 12.0$ and an IMF with $\alpha = 2.35$. In runs 8 and 9, the binaries always comprised of two $0.8393M_\odot$ main-sequence stars, whereas in runs 7 and 10, the masses were drawn from the IMF, as described earlier. In runs 7 and 8 we evolved the binaries up to a time of 15 Gyr, whereas in runs 9 and 10 we evolved the binaries until one of the events described in §5.5 occurred. Comparing run 7 to run 4, we see only a slight increase in the number of LMXBs produced. There are 28 additional unresolved binaries. In other words, we have produced fewer objects containing neutron stars in smothered or contact systems in run 7 compared to run 4. It is also important to note that the ratio of LMXBs to smothered systems is also quite different between runs 4 and 7. In the former many more smothered systems are produced. Comparison between runs 7 and 10 show that if we are willing to wait long enough, we are eventually left with more neutron stars in contact or smothered systems. The number of neutron stars merging with white dwarfs is particularly enhanced, as is the number of white dwarf/white dwarf mergers. Comparison of runs 7 and 10, to 8 and 9, show that binaries containing more massive stars tend to lead to fewer unresolved binaries (comparing runs 7 and 8), and a boost in the production of blue stragglers.

5.9 The Effect of Changing α_{ce}

In runs 11-13, we investigate the effects of changing the value of the efficiency of the common envelope stage, α_{ce}. As mentioned earlier, it has been suggested that $\alpha_{ce} \sim 0.2 - 0.4$. In our previous runs, we have assumed $\alpha_{ce} = 0.4$, in runs 11, 12, and 13 we took $\alpha_{ce} = 0.2$, 0.1, and 0.05, respectively. In all three runs, we use the cluster model with $W_0 = 12.0$, and $\alpha = 2.35$. We inject the binaries at a random time between zero and 15 Gyr, and evolve the binaries up to the present time (15 Gyr). We treat smothered neutron stars in the same way as runs 7 - 10, i.e. assuming the envelopes expand to engulf the binary companion. The binaries are selected in the same way as run 4.

Decreasing the value of α_{ce} has the following effect: the number of unresolved binaries decreases, as CE phases leave the two stars much closer together. In the case of two compact objects they are sufficiently close to merge via gravitational radiation inspiral (hereafter denoted as MGRI) in
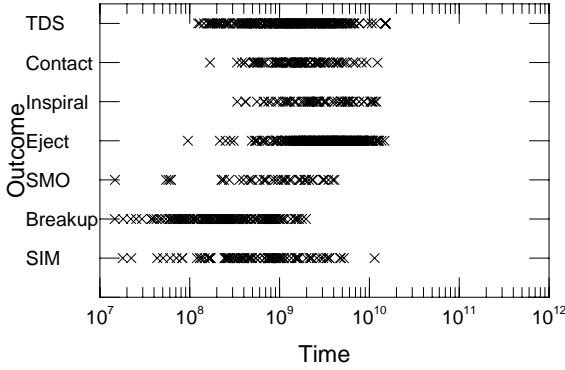
Figure 8. Final outcome of the binaries evolved in Run 17 (labelling same as Fig. 7).

more systems, hence we see a higher rate of such mergers. However, we note that the effect is relatively small: a factor of three between run 7 ($\alpha_{ce} = 0.4$) and run 13 ($\alpha_{ce} = 0.05$). The production rate of blue stragglers is seen to be independent of α_{ce}.

5.10 Production Rates for a More-concentrated Cluster

We now consider encounters in a more concentrated cluster, where $W_0 = 16.0$. Run 14 uses the same parameters as run 13, except for the cluster model. Comparing these two runs, we note that the number of unresolved binaries is greatly reduced in run 14 as the encounter timescale is much shorter because of the denser cluster core. The number of MGRI events is also much larger in run 14. Owing to the higher concentration, the more collapsed cluster has much higher mass segration, and thus the core contains a larger fraction of neutron stars. It therefore comes as no surprise to see a larger fraction of the MGRIs containing neutron stars in run 14 than run 13. The number of blue stragglers produced in both runs are comparable.

In run 15, we repeat the conditions of run 14, except we use $\alpha_{ce} = 0.4$. This has the effect of reducing the number of MGRIs produced and slightly increasing the number of unresolved binaries, as two stars are left further apart after a CE phase.

Run 16 is a repeat of run 15, except the evolution is halted as soon as a smothered neutron star in produced (the outcome being labelled "TDS" as before). From 1000 binaries, some 220 smothered neutron stars are produced. Including the MGRI events, the ratio of smothered neutron stars to LMXBs is ~ 10 in run 16, compared to ~ 3 in run 15. Clearly deciding how smothered neutron stars evolve is a crucial question in computing the ratio of LMXBs to other systems containing neutron stars.

In run 17, we repeat run 16, except we inject all the binaries into the cluster core at a time of zero. This has the effect of greatly reducing the number of unresolved binaries. The number of ejected binaries increases, as does the number

of smothered neutron stars. However, the number of MGRIs and contact binaries remains essentially the same as for run 16. In Figure 8 we plot the final outcomes of the binaries in run 17 as a function of time. Comparison with Figure 7 makes it clear that the evolutionary timescale for binaries in the more-concentrated cluster is significantly shorter, with all binaries reaching some end state in $< 10\,\mathrm{Gyr}$.

Finally, in runs 18–20 we investigate the effect on production rates of changing the IMF. Runs 18 and 19 are repeats of run 16, except we use IMFs with $\alpha = 2.0$, and 2.7, respectively. As was the case for the cluster model with $W_0 = 12.0$, the number of blue stragglers produced is a sensitive function of α; the number of blue stragglers being produced ranging from ~ 100 to ~ 230. The ratio of LMXBs to CVs is also seen to vary with α; a larger α implies a smaller number of neutron stars relative to white dwarfs and thus the ratio of LMXBs to CVs is reduced. In run 20, we repeat run 18, but do not halt the evolution of the binary when a smothered neutron star is produced. Comparison of run 20 to run 18 shows a decrease of the ratio of smothered neutron stars to LMXBs.

5.11 Production Rates for Less-concentrated Clusters

We now consider less-contrated clusters. In runs 21-23, we take the conditions of run 16, except that we use three different models for less-concentrated clusters, having $W_0 = 8.0$, 6.0, and 4.0 respectively. In all three runs, the lower density of stars leads to a much longer timescale for encounters compared to the denser clusters considered earlier. The vast majority of the 1000 binaries remain unresolved. The number of blue stragglers produced is seen to decrease steadily with decreasing core density. Only a handful of contact binaries are produced in the three runs, and no MGRI events occurred.

5.12 Comparison of 2+1 to 1+1 Rates

We now compare the production rates of astrophysically interesting objects by 2+1 encounters to those from encounters between two single stars, listed for the various cluster models in Table 9. The encounter rates listed in Table 9 are given in units of encounters/10^8 years, hence assuming the globular clusters are 15 Gyr old, we must multiply these numbers by 150 to obtain the total number produced (on our assuption that the population of single stars is static). In considering encounters between binaries and single stars, we injected 1000 binaries into the cluster cores. We must now consider how many binaries we expect to find in the cores of the various models. In the introduction, we stated that 2+1 encounters will be more important than 2+2 encounters provided that the mass fraction contained in binaries was small. Indeed in modelling the clusters as King-Mitchie models we neglected the effects of the binaries on the distribution of stars within the cluster. If we make the simple assumption that at a given time, $\sim 10\%$ of the stars in the core are contained in binaries, then we conclude from Table 8 that cluster models A-C contain ~ 1000-1500 binaries at any given time. For models D-F, the number is in the range 500-700, and for clusters G, H, and I, the numbers of binaries are 2500, 2000, and 1300 respectively. We now have to

Table 11. The total number of systems produced over 15 Gyr, via both single star/single star (1+1), and binary/single star (2+1) encounters.

Model	BS		NS			WD			MGRI	
	1+1	2+1	1+1	XB	SN	1+1	CV	SW	NW	WD$_a^2$
A	50	130	100	22	105	140	20	15	5	11
B	165	240	80	9	67	248	32	17	11	8
C	340	350	44	10	35	295	38	32	2	6
D	36	190	340	54	448	188	24	4	38	18
E	223	400	478	44	440	673	58	18	68	58
F	731	670	385	26	328	1278	98	66	70	110
G	35	160	14	2	4	41	4	14	0	0
H	18	80	1	0	0	9	0	0	0	0
I	7	20	0	0	0	3	1	0	0	0
B$'$	165	220	80	17	2	248	24	11	31	35
E$'$	223	374	478	48	4	673	62	18	276	84

BS is the number of blue stragglers produced. Under NS we list the number of neutron stars involved in 1+1 encounters, the number forming X-ray binaries (XB) via 2+1 encounters, and those in smothered systems formed via 2+1 encounters. We list the equivalent three numbers for white dwarfs under WD, with CV standing for cataclysmic variables. As in Table 10, systems brought into contact via gravitational radiation are labelled MGRI (mergers through gravitational radiation inspiral). Here we subdivide this outcome into: neutron star/white dwarf mergers (NW), and white dwarf/white dwarf mergers where the total mass is greater than the Chandrasekhar mass (WD$_a^2$). In models B$'$ and E$'$, we treat the evolution of a smothered neutron star in a binary in the same way as for white dwarfs and assume the envelope expands engulfing the other binary component and leading to a common envelope phase. We also take the common envelope efficiency $\alpha_{ce} = 0.05$ rather than the value used in the other runs listed ($\alpha_{ce} = 0.4$).

consider the average time taken by a binary injected into a core to reach one of the end states (*i.e.* ejection, merging *etc*). For cluster models A-C, inspection of Table 10 (runs 4-6) reveals that ~ 500 of the original 1000 binaries have reached some end state in 15 Gyr. For models D-F, this number is $\sim 0 - 200$. In fact, in these more collapsed clusters, $\sim 50\%$ of the binaries have reached some end state in $\sim 1-2$ Gyr. Hence for cluster models D-F, we might imagine that in 15 Gyr, the core is able to "process" $\sim 2000 - 4000$ binaries. In all other cases, our assumptions here seem to suggest that the cores will be unable to deal with more than 1000 binaries. In the case of models G-I, only a very small fraction of injected binaries will reach some end state, as seen in Table 10. In other words when comparing the rates for encounters between two single stars given in Table 8 to those for encounters between single stars and binaries given in Table 10, we should apply the following factors to the latter: ~ 1 for models A-C, $\sim 2 - 4$ for models D-F, and $\sim 1 - 2$ for models G-I. Assuming encounters happen at a uniform rate over 15 Gyr, we should then multiply the rates in Table 9 by a factor of 150.

In Table 11, we list the total expected production of blue stragglers and systems containing compact objects, assuming the adjustment factors discussed in the previous paragraph. Considering first the production of blue stragglers, we see that the ratio of the number produced via 2+1 encounters to the number produced via 1+1 encounters is a sensitive function of cluster concentration and IMF. In models

A-C, roughly equal numbers of blue stragglers are produced through both pathways. We note again that a larger value of the IMF power law, α, implies a greater mass fraction contained in main-sequence stars, which leads to an increase in the production of blue stragglers. We now consider the most concentrated clusters, models D-F. In model D, we produce very few blue stragglers from 1+1 encounters. We have a relatively flat power-law IMF, and the lower-mass main-sequence stars have been largely excluded from the core by the effects of mass segregation. In models E and F, the steeper power-law IMF, means more main-sequence stars remain in the core, and the number of blue stragglers produced are larger than for models B and C because of the increased density. By comparison, the number of blue stragglers produced via 2+1 encounters show less variation between models D-F. In models D and E, the number of 2+1 events is greater than the number of 1+1 events, whereas for model F, the two numbers are comparable. Finally, looking at the least concentrated clusters considered, namely models G-I, we see that 2+1 encounters are significantly more important than 1+1 encounters in producing BSs in low-density clusters. We also note that in models B$'$ and E$'$ in Table 11, we have changed the way we deal with smothered neutron stars contained in binaries, treating them exactly the same as white dwarfs. One would expect this to have little effect on the production of BSs, an expectation seen in the results.

We next consider the number of systems produced con-

taining neutron stars. Looking first at models A-C, we see that the number of neutron stars involved in 1+1 encounters is roughly equal to those in X-ray binaries or smothered systems produced from 2+1 encounters. Both numbers show a strong dependence on the IMF power law, α, with a flatter IMF leading to an increase in the number of systems produced. We note also that the number of systems brought into contact via gravitational radiation is relatively small. If we assume systems produced via 1+1 encounters all form smothered systems, then our ratio of smothered systems to X-ray binaries $\sim$ 10:1. Considering next the most-concentrated clusters, models D-F, we see that the number of systems produced has increased compared to models A-C owing to the greater densities and increased core mass fraction contained in neutron stars due to stronger mass segregation effects. We also note that the number of MGRI systems has increased; owing to the shorter encounter timescale in the densest cores, systems pass through a common envelope stage at an earlier time, and thus have more time to spiral together. If we include all neutron star/white dwarf and white dwarf/white dwarf (with total mass above the Chandrasekhar limit) coalescences in the total number of smothered neutron star systems, then this number will be enhanced by 10–60 % for models D-F. With the same assumptions as above, we expect the ratio of smothered systems to X-ray binaries $\sim$ 15:1 for model D, and $\sim$ 30 : 1 for model F. We thus see that it is quite possible that a much larger number of systems are produced containing smothered neutron stars. If these systems evolve into MSPs, they may do so without passing through a prolonged phase of X-ray emission, hence we would not expect to see roughly equal numbers of LMXBs and MSPs in globular clusters. Assuming that LMXBs have a lifetime $\sim$ 1Gyr, then we would expect to see $\sim 1 - 3$ LMXBs in cluster models A-F. Let us now consider models B$'$ and E$'$. As mentioned earlier, in these runs we treated smothered neutron stars in binaries in a similar way to smothered white dwarfs, assuming their gaseous envelopes expanded to engulf the other component of the binary to enter a common envelope phase. In order to maximise the number of MGRI products, we considered a relatively low value for the common envelope efficiency, $\alpha_{ce} = 0.05$, which will leave post-CE phase stars closer together than larger values. We note that the number of X-ray binaries is increased slightly (comparing B$'$ to B, and E$'$ to E). The total number of smothered systems produced via 2+1 encounters is reduced only slightly though this result is very dependent on the value of α_{ce}. The ratio of smothered systems to X-ray binaries $\sim$ 10 : 1 for model B$'$, and $\sim$ 20 : 1 for model E$'$, these ratios being reduced by a factor of two when α_{ce} is increased to 0.4. Hence we see the importance of determining the subsequent evolution of smothered neutron stars, and calculating the value of α_{ce}.

We should remind ourselves of the uncertainty in the outcomes of encounters between a neutron star and a main-sequence star. In the ratios computed above, we have assumed that all such encounters will produce smothered neutron stars. In previous work (Davies, Benz & Hills [1992]), we showed that at least $\sim$ 0.5 of the encounters between single main-sequence and neutron stars would produce smothered systems. If only one half actually did so, then the ratio of smothered systems to X-ray binaries $\sim$ 5 : 1 for models A-C, with similar reductions in the other models. Hence we conclude two things: 1) the fraction of single encounters producing clean binaries would be a useful number to determine, and 2) even if half such encounters produce clean binaries we still seem likely to produce a much larger number of smothered systems, the pessimistic factor of five mentioned here possibly representing a useful step towards explaining the excess of MSPs compared to LMXBs as seen in globular clusters today.

Finally, we consider the number of systems produced containing white dwarfs. In some sense, comparison of the 1+1 to the 2+1 rates is misleading, as we have assumed in all 2+1 runs that a smothered white dwarf in a binary will essentially form a red giant and engulf the other companion to form a common envelope system. If we assume that none of the systems produced via 1+1 encounters will produced CVs, then we conclude that the number of CVs will be very much smaller than the number of smothered white dwarfs produced for models A-F. We expect the smothered white dwarfs to evolve to form red giants; the compact object accreting material as the envelope expands. In the case of the most-massive white dwarfs smothered by the remains of a main-sequence star, it is possible that it will accrete enough material to exceed the Chandrasekhar mass, possibly forming a neutron star via AIC. The number of white dwarf/white dwarf mergers occuring via gravitational radiation inspiral where the total mass is *less* than the Chandrasekhar limit is negligible for all models.

REFERENCES

Binney J. J., Tremaine S., 1987, in Galactic Dynamics. Princeton, p.235
Cannon R. C., 1993, MNRAS, 263, 817
Cleary P. W., Monaghan J. J., 1990, ApJ, 349, 150
Davies M. B., Benz W., Hills J. G., 1992, ApJ, 401, 246
Davies M. B., Benz W., Hills J. G., 1993, ApJ, 411, 285
Davies M. B., Benz W., Hills J. G., 1994, ApJ, 424, 870
DiStefano R., Rappaport S. A., 1992, ApJ, 396, 587
Grabhorn R. P., Cohn H. N., Lugger P. M., Murphy B. W., 1992, ApJ, 392, 86
Hut P., McMillan S., Romani R. W., 1992, ApJ, 389, 527
Hut P., Verbunt F., 1984, Nature, 301, 587
Iben I. Jr., Renzini A., 1983, ARA&A, 21, 271
Kochanek C. S., 1992, ApJ, 385, 604
Krolik J., 1984, ApJ, 282, 452
Lightman A. P., Shapiro S. L., 1977, ApJ, 211, 244
Meylan G., 1987, A&A, 184, 144
Meylan G., 1989, A&A, 214, 106
Phinney E. S. P., Kulkarni S., 1994, ARA&A, 32, 591
Pryor N., Meylan G., 1993, in Djorgovski S. G., Meylan G., eds, ASP Conference Series vol. 50: Structure and Dynamics of Globular Clusters. p.357
Sigurdsson S., Phinney E. S. P., 1994, ApJ, submitted
Taam R. E., Bodenheimer P., 1989, ApJ, 337, 849
Verbunt F., Zwaan C., 1981, a&a, 100, L9